Journal of Sound and Vibration (2000) **230**(3), 661–688
doi.10.1006/jsvi.1999.2650, available online at http://www.idealibrary.com on IDEAL®

DESIGN, THEORY AND VALIDATION OF A LOW MASS 6-d.o.f. TRANSDUCER

L. IVARSSON AND M. A. SANDERSON*

Department of Applied Acoustics, Chalmers University of Technology, S-412 96 Gothenburg, Sweden

AND

A. G. TROSHIN

Krylov Shipbuilding Research Institute, St. Petersburg 196158, *Russia*

(*Received* 12 *May* 1998, *and in final form* 2 *September* 1999)

The need for measuring multidirectional responses is becoming increasingly important in applications such as modal analysis, verification of dynamic models, etc. Therefore, a transducer comprised of a fixture containing six linear accelerometers has been developed and tested in order to measure six degrees of freedom at a point. The term transducer in this context includes both the fixture and the six accelerometers. In order to minimize the loading of the measurement object, the weight of the transducer is kept small by using low weight accelerometers and a hollow aluminum fixture. At the same time, the transducer is designed sufficiently stiff in order to consider it as a rigid body for use up to approximately 600 Hz. For the motion of the transducer, systems of equations are derived which include the transverse sensitivities of the six accelerometers. The influence of the transverse sensitivity is investigated in a parameter study on a structure consisting of a three-dimensional beam structure, excited in such a way that motion results in all directions. The transducer design leads to two important measurement features; a centrally located hole in order to measure and excite driving point frequency response functions and a flat surface in order to measure close to the surface of the structure. Experimental results are compared with theoretical ones. It was found that the major limitation of the transducer results from the inherent transverse sensitivities of the accelerometers.

1. INTRODUCTION

The measurement of the angular or rotational degrees of freedom (d.o.f.) of motion is often necessary as a complement to the translational d.o.f.s in vibration analyses. The rotational d.o.f.s have found use in, among others, the following applications: modal analysis [1], dynamic analysis of connected structures [2], vibration isolation [3], analysis and control of vibrational power transmissions to machinery supporting structures [4, 5] in which concentrated excitation on structures is discussed.

*Now at: Lear Corporation, 21557 Telegraph Road, Southfield, MI 48034-4248, USA.

0022-460X/00/080661 + 28 $35.00/0

Various techniques have been developed to obtain the rotational response. In reference [6] the angular motion was estimated from the linear motion of the test structure. In references [7, 8] the angular motion for one d.o.f. was estimated using accelerometer pairs. Special transducers for measuring the angular motion in one direction have been developed, see for example reference [9], and non-contacting methods using laser techniques have also been tested, and see for example reference [10]. In reference [11] a 6-d.o.f. translational–rotational, cube-shaped sensor was examined.

In this work, a low mass, thin, six d.o.f.s triangular-shaped transducer, comprised of a fixture containing six ordinary accelerometers is configured and tested. Usually, at most, three translational d.o.f.s are measured at points on structures and the rotational d.o.f.s are neglected because they are said to be difficult to measure or not considered important. The 6-d.o.f. transducer is therefore configured to measure the three translational and the three rotational d.o.f.s of motion at a point simultaneously. To reduce the effects of loading, the transducer is designed with a low mass, approximately 6 g.

In order to measure the response as near as possible to the surface of the measurement object, the 6-d.o.f. transducer is kept thin. The transducer has a centrally located hole so that the structure can be excited with the excitation and response points coinciding. Each accelerometer on the 6-d.o.f. transducer has a mass of 0·2 g and a maximum transverse sensitivity ranging from 0·3 to 0·8%.

2. THEORY, 6 d.o.f.s OF MOTION

The estimation of the translational, a, and the rotational, α, accelerations by using two linear accelerometers located at points A and B separated by distance $2L$ is depicted in Figure 1. The translational and rotational accelerations at the origin, o, are approximated respectively as

$$a_o = (a_A + a_B)/2 \quad \text{and} \quad \alpha_o = (a_A - a_B)/2L. \tag{1, 2}$$

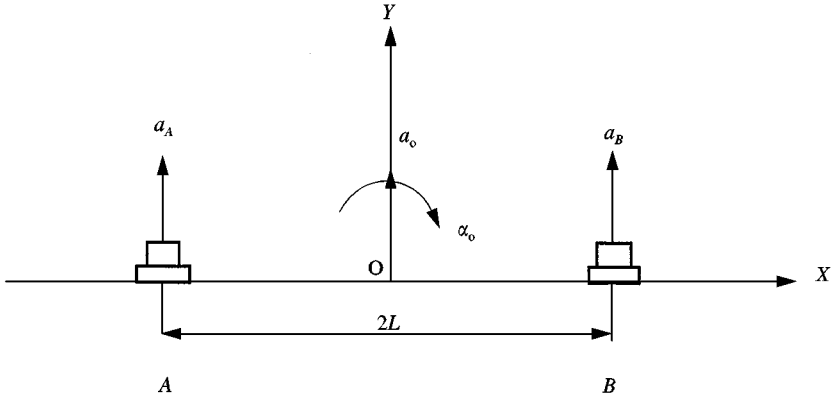

Figure 1. Measurement of the rotational and translational responses at the origin, O, using two accelerometers located points A and B, separated by distance $2L$.

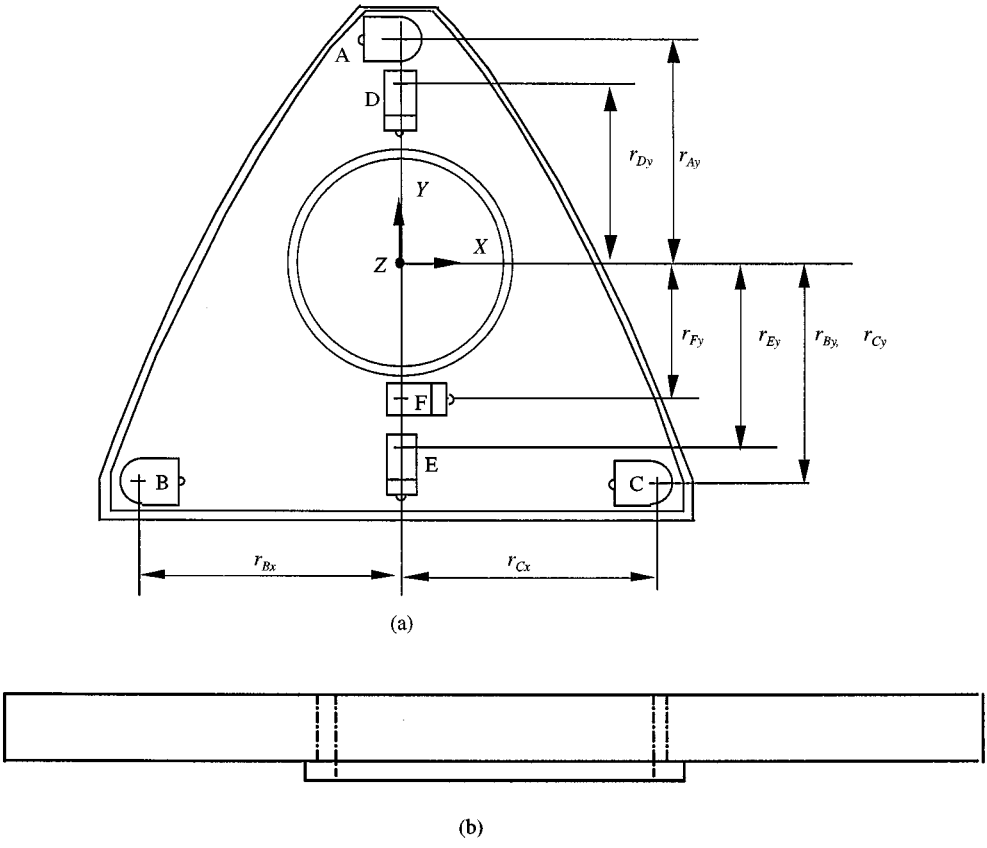

Figure 2. (a) Top view of the 6-d.o.f. transducer showing the linear accelerometers marked A–F and distances, r, to the center, (b) side view of the 6-d.o.f. transducer.

The accelerometers can be placed directly on the structure or mounted on a fixture which is attached to the structure; see for example reference [7].

However, this is a simplified description since it is a finite difference approximation and motion in the other four d.o.f.s is not included as well as the transverse sensitivities of the accelerometers. Upon assuming the 6-d.o.f. transducer behaves as a rigid body in motion, the ordinary equations for kinematic analyses of rigid bodies can be used. The geometry of the 6-d.o.f. transducer with the six accelerometers A to F is shown in Figures 2(a) and 2(b). In order to achieve a stiff and low mass design, the transducer is built as a closed triangular box with a hole in the center. The fixture for the accelerometers is made of aircraft aluminum and has the following material properties: Young's modulus $E = 0{\cdot}72$ GPa, density $\rho = 2700$ kg/m^3 and a shell thickness of about 0·5 mm and was manufactured from a solid block. The origin of the co-ordinate system is located in the center of this hole: i.e., the point where the translational and the rotational d.o.f.s are calculated by using combinations of the six accelerometers. The distances between the center of the transducer and each accelerometer are marked, r, with different indices depending on accelerometer location.

3. RIGID-BODY DYNAMICS INCLUDING TRANSVERSE-SENSITIVITY

When using piezo-electric accelerometers there exists many factors that can lead to measurement problems such as base bending, X-rays, γ-rays, high and low temperatures, temperature fluctuations, humidity, electromagnetic fields, high sound levels, poor mounting and transverse vibrations; see for example reference [13].

In the following, the errors due to transverse vibrations will be studied in more detail because they can cause large errors depending on the motion of the structure and the value of the transverse sensitivity of the accelerometer which is an inherent property of all piezo-electrical accelerometers.

The accelerometers that comprise the 6-d.o.f. transducer in this work are of ICP-type and contain piezo-crystals.

When using accelerometers containing a piezo-crystal, there exists one direction which provides the maximum sensitivity defined by θ and ϕ, i.e., charge output/unit acceleration which is called H_{max}. The sensitivity, H_z along the z-axis or in the measurement direction is $H_{max}\cos(\theta)$. For a perfect piezo-transducer the vertical axis (z-axis in Figure 3) would coincide with this H_{max}-axis. Due to manufacturing tolerances and crystal element variations, they do not coincide and the accelerometer acquires a transverse sensitivity. The projection of the H_{max}-vector on the x–y plane gives a new vector T, which can be divided into components, T_x, in the x direction and, T_y, in the y direction; see Figure 3.

This means that the sensitivity of an accelerometer, using piezo-elements, can be described as having one main direction and two transverse sensitivity directions. For example, see Figures 4(a) and 4(b), containing the transverse sensitivities for accelerometer positions A to F.

As seen in Figure 4(a) accelerometer A, for example, has a main sensitivity, H_{Az}, in the Z direction and the transverse sensitivities, T_{Az} and T_{Ay}, in the X and

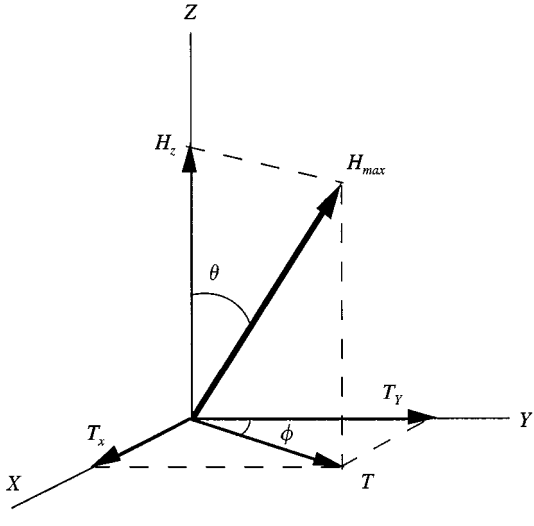

Figure 3. Transverse sensitivity of a piezoelectric accelerometer.

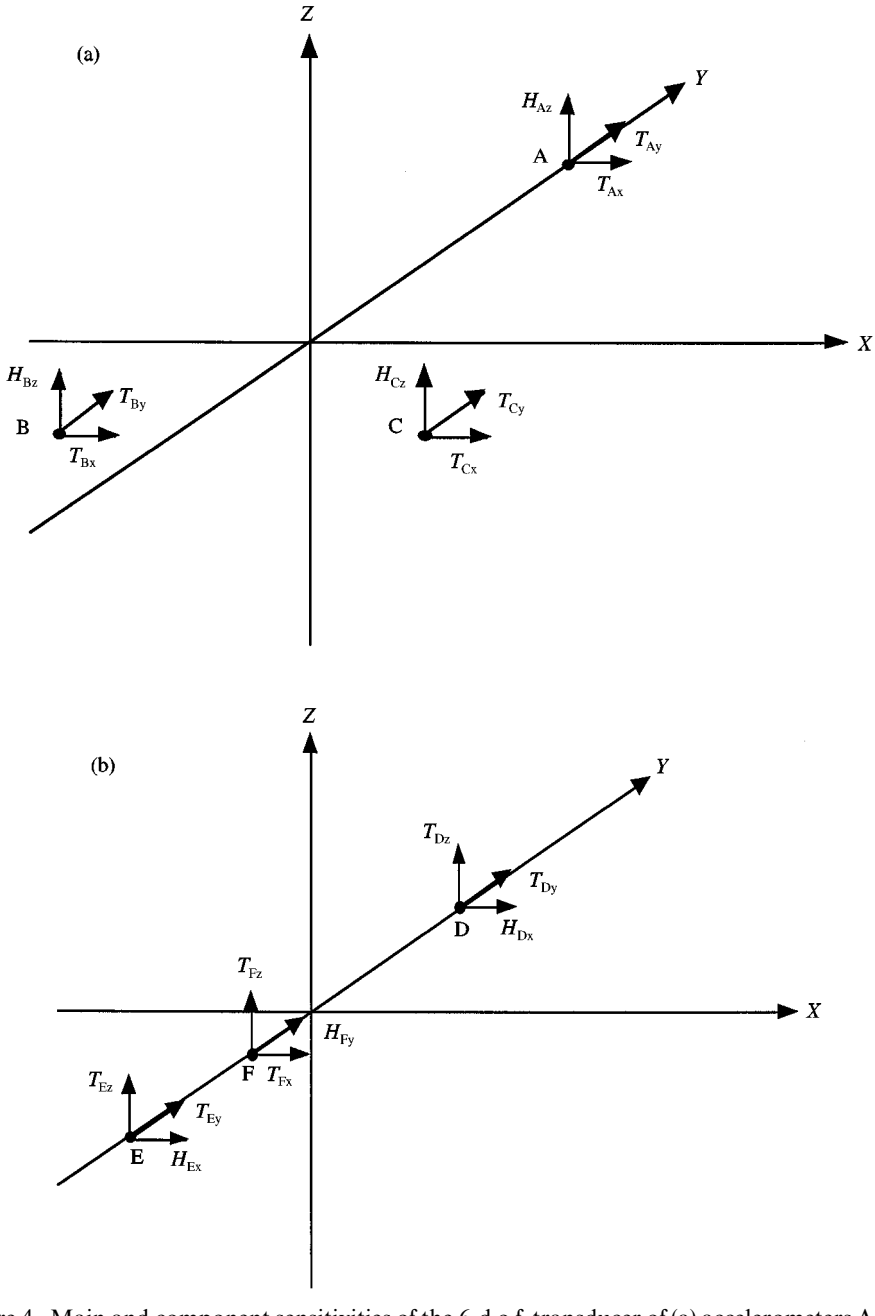

Figure 4. Main and component sensitivities of the 6-d.o.f. transducer of (a) accelerometers A, B and C and (b) accelerometers D, E and F.

Y directions. The measured acceleration, for example, a_{Azm} contains the transverse sensitivities T_{Ax} and T_{Ay} expressed as

$$a_{Azm} = a_{Az}H_{Az} + a_{Ax}T_{Ax} + a_{Ay}T_{Ay}. \tag{3}$$

The accelerations at the origin of the transducer can be found by using the ordinary equations for kinematic analyses of rigid bodies. Including the transverse sensitivity of the accelerometers in expressions similar to equation (3) gives the 6-d.o.f.s responses at a point as

$$\begin{aligned} a_{oxm} = {} & (a_{Ex} r_{Dy} H_{Ex} + a_{Dx} r_{Ey} H_{Dx} + a_{Oy} r_{Ey} T_{Dy} + a_{Oz} r_{Ey} T_{Dz} + a_{Oy} r_{Dy} T_{Ey} + a_{Oz} r_{Dy} T_{Ez} \\ & - r_{Dy} r_{Ey} T_{Dy} \omega_x^2 + r_{Dy} r_{Ey} T_{Ey} \omega_x^2 + r_{Dy} r_{Ey} T_{Dz} \dot{\omega}_x - r_{Dy} r_{Ey} T_{Ez} \dot{\omega}_x + r_{Dy} r_{Ey} T_{Dz} \omega_y \omega_z \\ & - r_{Dy} r_{Ey} T_{Ez} \omega_y \omega_z - r_{Dy} r_{Ey} T_{Dy} \omega_z^2 + r_{Dy} r_{Ey} T_{Ey} \omega_z^2)/(r_{Dy} + r_{Ey}), \end{aligned} \tag{4}$$

$$a_{oym} = a_{Fy} H_{Fy} + a_{Fx} T_{Fx} + a_{Fz} T_{Fz} - r_{Fy} \omega_x^2 - r_{Fy} \omega_z^2, \tag{5}$$

$$\begin{aligned} a_{ozm} = {} & (a_{Bz} r_{Ay} H_{Bz} + a_{Cz} r_{Ay} H_{Cz} + 2 a_{Az} r_{By} H_{Az} + 2 a_{Ox} r_{By} T_{Ax} + 2 a_{Oy} r_{By} T_{Ay} \\ & + a_{Ox} r_{Ay} T_{Bx} + a_{Oy} r_{Ay} T_{By} + a_{Ox} r_{Ay} T_{Cx} + a_{Oy} r_{Ay} T_{Cy} - 2 r_{Ay} r_{By} T_{Ay} \omega_x^2 \\ & + r_{Ay} r_{By} T_{By} \omega_x^2 + r_{Ay} r_{Cy} T_{Cy} \omega_x^2 + 2 r_{Ay} r_{By} T_{Ax} \omega_x \omega_y - r_{Ay} r_{By} T_{Bx} \omega_x \omega_y \\ & - r_{Ay} r_{Bx} T_{By} \omega_x \omega_y - r_{Ay} r_{Cy} T_{Cx} \omega_x \omega_y + r_{Ay} r_{Cx} T_{Cy} \omega_x \omega_y + r_{Ay} r_{Bx} T_{Bx} \omega_y^2 \\ & - r_{Ay} r_{Cx} T_{Cx} \omega_y^2 - 2 r_{Ay} r_{By} T_{Ay} \omega_z^2 + r_{Ay} r_{Bx} T_{Bx} \omega_z^2 + r_{Ay} r_{By} T_{By} \omega_z^2 - r_{Ay} r_{Cx} T_{Cx} \omega_z^2 \\ & + r_{Ay} r_{Cy} T_{Cy} \omega_z^2 - 2 r_{Ay} r_{By} T_{Ax} \dot{\omega}_z + r_{Ay} r_{By} T_{Bx} \dot{\omega}_z - r_{Ay} r_{Bx} T_{By} \dot{\omega}_z \\ & + r_{Ay} r_{Cy} T_{Cx} \dot{\omega}_z + r_{Ay} r_{Cx} T_{Cy} \dot{\omega}_z)/(2(r_{Ay} + r_{By})), \end{aligned} \tag{6}$$

$$\begin{aligned} \dot{\omega}_{xm} = {} & (2 a_{Az} H_{Az} - a_{Bz} H_{Bz} - a_{Cz} H_{Cz} + 2 a_{Ox} T_{Ax} + 2 a_{Oy} T_{Ay} - a_{Ox} T_{Bx} - a_{Oy} T_{By} \\ & - a_{Ox} T_{Cx} - a_{Oy} T_{Cy} - 2 r_{Ay} T_{Ay} \omega_x^2 - r_{By} T_{By} \omega_x^2 - r_{Cy} T_{Cy} \omega_x^2 + 2 r_{Ay} T_{Ax} \omega_x \omega_y \\ & + r_{By} T_{Bx} \omega_x \omega_y + r_{Bx} T_{By} \omega_x \omega_y + r_{Cy} T_{Cx} \omega_x \omega_y - r_{Cx} T_{Cy} \omega_x \omega_y - r_{Bx} T_{Bx} \omega_y^2 \\ & + r_{Cx} T_{Cx} \omega_y^2 - 2 r_{Ay} \omega_y \omega_z - 2 r_{By} \omega_y \omega_z - 2 r_{Ay} T_{Ay} \omega_z^2 - r_{Bx} T_{Bx} \omega_z^2 - r_{By} T_{By} \omega_z^2 \\ & + r_{Cx} T_{Cx} \omega_x^2 - r_{Cy} T_{Cy} \omega_z^2 - 2 r_{Ay} T_{Ax} \dot{\omega}_z - r_{By} T_{Bx} \dot{\omega}_z + r_{Bx} T_{By} \dot{\omega}_z - r_{Cy} T_{Cx} \dot{\omega}_z \\ & - r_{Cx} T_{Cy} \dot{\omega}_z)/(2(r_{Ay} + r_{By})), \end{aligned} \tag{7}$$

$$\begin{aligned} \dot{\omega}_{ym} = {} & (a_{Bz} H_{Bz} - a_{Cz} H_{Cz} + a_{Ox} T_{Bx} + a_{Oy} T_{By} - a_{Ox} T_{Cx} - a_{Oy} T_{Cy} + r_{By} T_{By} \omega_x^2 \\ & - r_{Cy} T_{Cy} \omega_x^2 - r_{By} T_{Bx} \omega_x \omega_y - r_{Bx} T_{By} \omega_x \omega_y + r_{Cy} T_{Cx} \omega_x \omega_y - r_{Cx} T_{Cy} \omega_x \omega_y \\ & + r_{Bx} T_{Bx} \omega_y^2 + r_{Cx} T_{Cx} \omega_y^2 + 2 r_{Bx} \omega_x \omega_z + r_{Bx} T_{Bx} \omega_z^2 + r_{By} T_{By} \omega_z^2 + r_{Cx} T_{Cx} \omega_z^2 \\ & - r_{Cy} T_{Cy} \omega_z^2 + r_{By} T_{Bx} \dot{\omega}_z - r_{Bx} T_{By} \dot{\omega}_z - r_{Cy} T_{Cx} \dot{\omega}_z - r_{Cx} T_{Cy} \dot{\omega}_z)/(2 r_{Bx}), \end{aligned} \tag{8}$$

$$\dot{\omega}_{zm} = (a_{Dx}H_{Dx} + a_{Ex}H_{Ex} - a_{Oy}T_{Dy} - a_{Oz}T_{Dz} + a_{Oy}T_{Ey} + a_{Oz}T_{Ez} + r_{Dy}T_{Dy}\omega_x^2$$

$$+ r_{Ey}T_{Ey}\omega_x^2 - r_{Dy}T_{Dz}\dot{\omega}_x - r_{Ey}T_{Ez}\dot{\omega}_x + 2r_{Dy}\omega_x\omega_y - r_{Dy}T_{Dz}\omega_y\omega_z$$

$$- r_{Ey}T_{Ez}\omega_y\omega_z + r_{Dy}T_{Dy}\omega_z^2 + r_{Ey}T_{Ey}\omega_z^2)/(2r_{Dy}). \quad (9)$$

Here the index m indicates a measured quantity, ω the angular velocity response and $\dot{\omega}$ the angular acceleration response.

4. THE IMPORTANCE OF TRANSVERSE SENSITIVITY

Expressions (4)–(9) are quite lengthy. The terms related to the transverse sensitivities can be divided into first order terms, containing accelerations and second order terms, containing angular velocities squared. The first order terms can be divided into two parts: part 1, which consists of an acceleration multiplied by a main sensitivity, and part 2 consisting of an acceleration multiplied by a transverse sensitivity. The second order term is called part 3 for simplicity.

In order to compare the importance of the three different parts of expressions (4)–(9), a special test structure was designed and analyzed both with the finite element (FE) method and compared with measurements.

The test structure consists of three steel beams of different lengths that are rigidly connected (welded) at the corner; see Figure 5. The test structure has the following

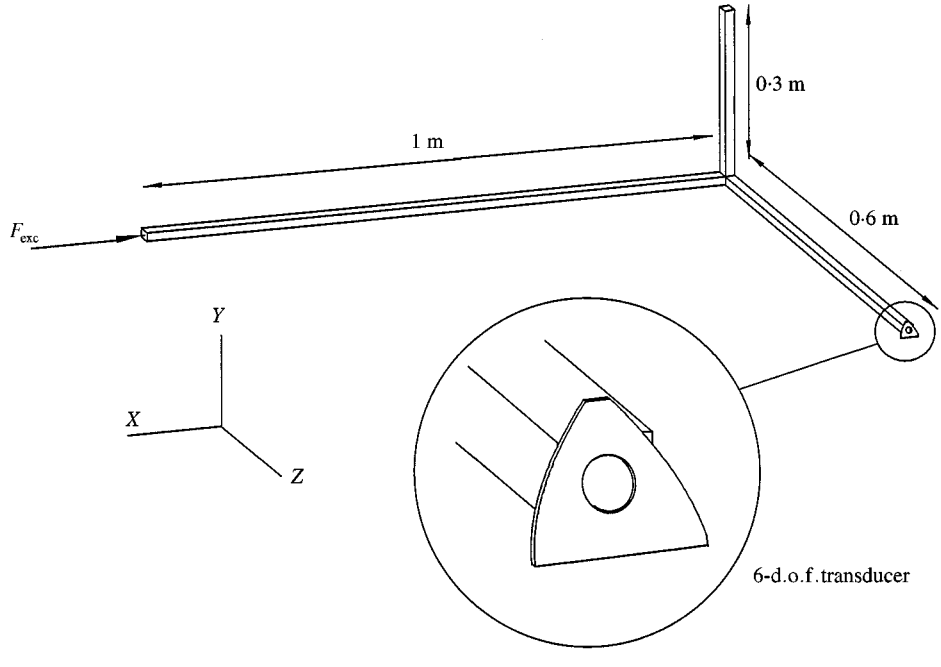

Figure 5. The test structure and positions of the force excitation and the 6-d.o.f. transducer.

properties: Young's modulus $E = 210\,\text{GPa}$, density $\rho = 7880\,\text{kg/m}^3$, structural damping $\eta = 0{\cdot}003$ and cross-section $0{\cdot}03 \times 0{\cdot}03\,\text{m}^2$.

The transducer is mounted on one beam end and a dynamic force in the x direction excites the test structure, while suspended in free conditions. Because of the geometry of the test structure, the point on the beam where the transducer is mounted has motion in all 6-d.o.f.s. To obtain theoretical data, the structure is also modelled in FE. The motion at the transducer position is easily calculated for this model. In this way, the behavior of accelerometers with different transverse sensitivity can be simulated.

Each accelerometer is considered to have a maximum sensitivity direction as shown in Figure 3. This maximum sensitivity vector, H_{max}, can, as mentioned previously, be divided into a main sensitivity vector, H_z, and transverse sensitivity components, T_x and T_y, which are the projections of the maximum sensitivity vector. In accelerometer specifications, the magnitude of the transverse sensitivity is given as a percentage of the magnitude of the maximum sensitivity (typically 2%). The direction of the maximum sensitivity vector is usually not given. This means that the transverse sensitivity components are not known. In a simple test for determining the transverse sensitivities, a laser doppler vibrometer was used to measure the responses of accelerometers driven by a shaker. However, the transverse sensitivity could not be determined; see Appendix A.

The direction of the maximum sensitivity vector depends on the orientation of the piezo-crystals and tolerances. Because of the fact that only the magnitude of the maximum sensitivity vector is known, the transverse sensitivity terms, T_x, and T_y,

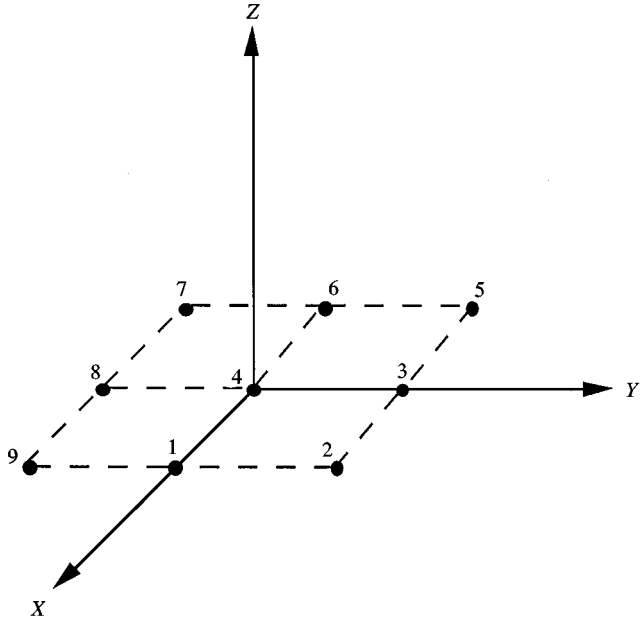

Figure 6. The nine end points of vector T.

can have different signs depending on the direction of the vector. Therefore, when analyzing the results of the transverse sensitivity, both negative and positive combinations of T_x and T_y must be taken into account.

When performing an estimation of the rotational or translational acceleration at the origin of the transducer, by using expressions (4)–(9), usually more than one accelorometer is involved. Each accelerometer has a maximum sensitivity direction that is independent of the other accelerometer's maximum sensitivity directions. Therefore, the directions and magnitudes of the responses from the different accelerometers are independent events.

Because the direction of the maximum sensitivity is not known the influence of the transverse sensitivity will give a different electrical output depending on how the accelerometer is mounted. Only those cases where the maximum sensitivity direction differs the most from the normal direction to the mounting surface were considered. These cases for each accelerometer can be seen in Figure 6 where the circles 1–9 represent the end points of the vector T. Point 4 is only significant when studying combinations of two or more accelerometers. It is easy to realize that if, for example, two accelerometers are used in the estimation there are 9^2 different combinations. For the case of estimating the angular acceleration, $\dot{\omega}_x$, in the x direction where information from three accelerometers are used there are 9^3 different combinations.

In order to analyze the importance of the transverse sensitivity, responses from FE calculations were used and "measurement" results were calculated by adding them according to expressions (4)–(9). This was then done for all significant combinations of transverse sensitivity as discussed before. However, a transverse sensitivity magnitude is needed for these calculations. The transverse sensitivity magnitude of an accelerometer is usually around 2–5% of the main sensitivity. Magnitudes below 0·5% are very difficult to achieve. In this study the magnitudes 0, 0·1, 1 and 3% were studied. In order to reduce the number of combinations, all accelerometers involved were assumed to have the same magnitude of transverse sensitivity. This is of course a simplification in comparison to real measurements when accelerometers of different transverse sensitivity magnitudes are used. However, setting all the transverse sensitivity magnitudes in the calculation to the same amount as the highest transverse sensitivity magnitude of the accelerometers used in the measurement, gives the maximum error for this case. The different transverse sensitivity magnitudes of the accelerometers can of course be included in a numerical study but would not add any greater understanding.

The mass and rotary inertia were not included in the FE calculations. However, FE studies show that inclusion of the mass and inertia of the transducer has a very small effect on the structure for the frequencies studied.

5. RESULTS FROM CALCULATIONS OF TRANSVERSE SENSITIVITY COMBINATIONS

In order to show the influence of these transverse sensitivities, the maximum and minimum level of the calculated responses for all combinations and at each

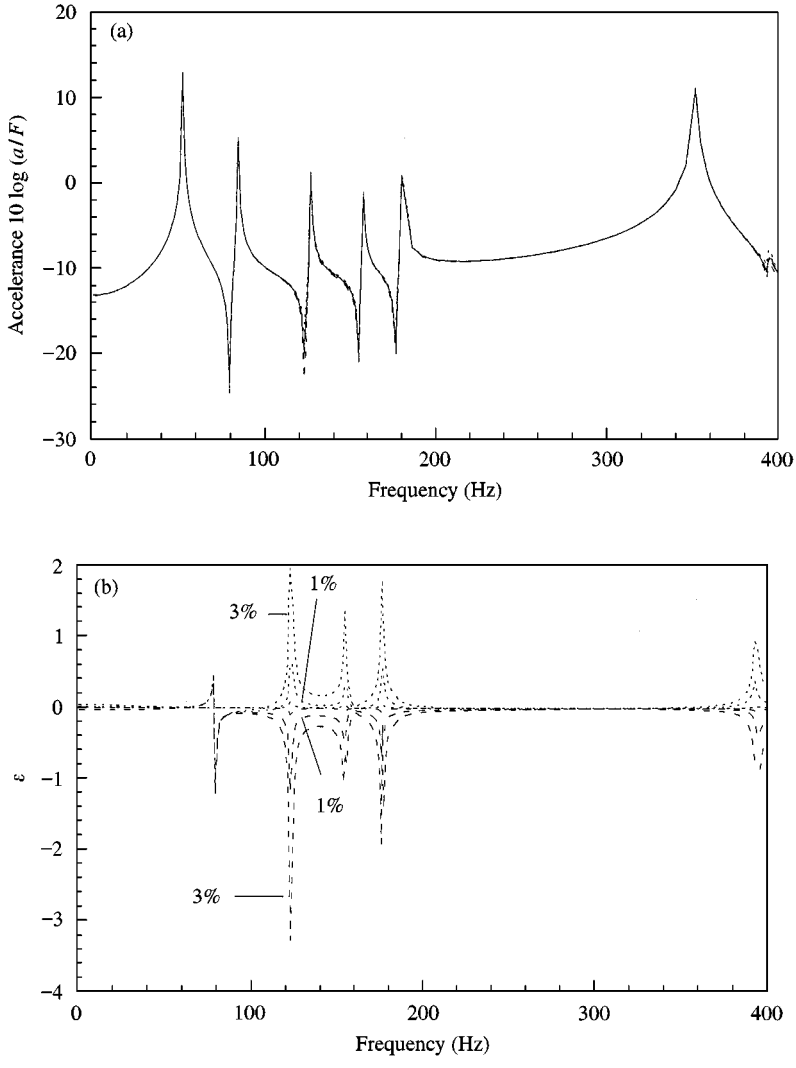

Figure 7. Influence of the transverse sensitivities on the accelerances : (—) 0%, (- - -) positive error and (– – –) negative error 0·1%, 1% and 3%; (a) x direction; (b) error in x direction; (c) y direction; (d) error in y direction; (e) z direction; (f) error in z direction; (g) $\dot{\omega}_x$ direction; (h) error in $\dot{\omega}_x$ direction; (i) $\dot{\omega}_y$ direction; (j) error in $\dot{\omega}_y$ direction; (k) $\dot{\omega}_z$ direction; (l) error in $\dot{\omega}_z$ direction. Both positive and negative errors are indicated for most sensitivities.

frequency are plotted in Figure 7. The responses are shown as accelerances for the 6-d.o.f.s. The case of there being no transverse sensitivities for all accelerometers is also included in these plots. For each response figure the resulting error is shown. The error is calculated as the level difference between the correct level (i.e., without transverse sensitivity) and the resulting maximum respective minimum accelerance level due to the different combination of transverse sensitivities.

As seen in Figure 7, the error due to the transverse sensitivity depends on the vibration amplitudes and is largest when the acceleration in the direction of interest

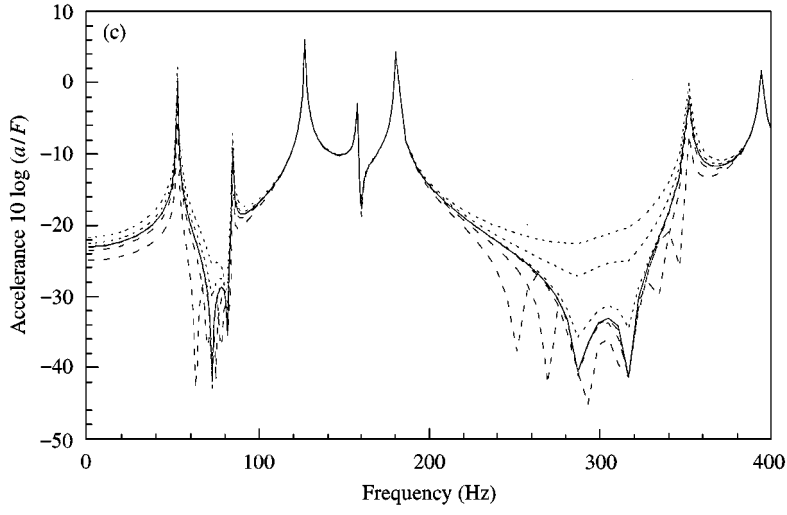

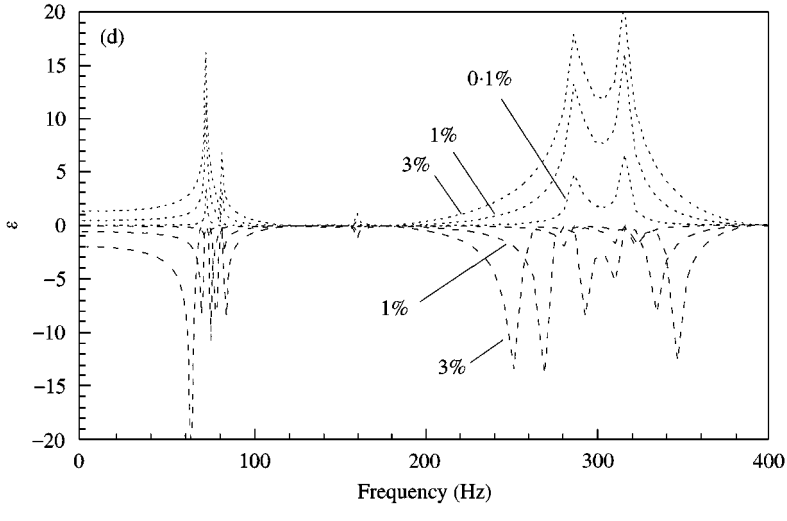

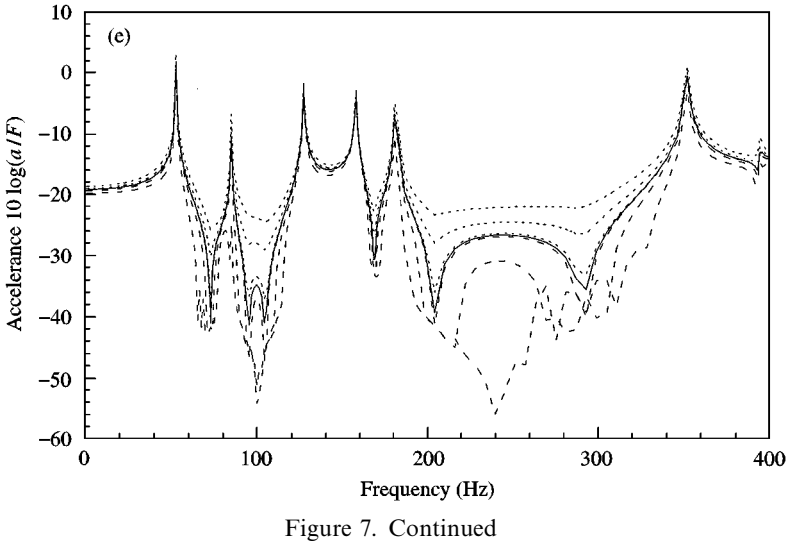

Figure 7. Continued

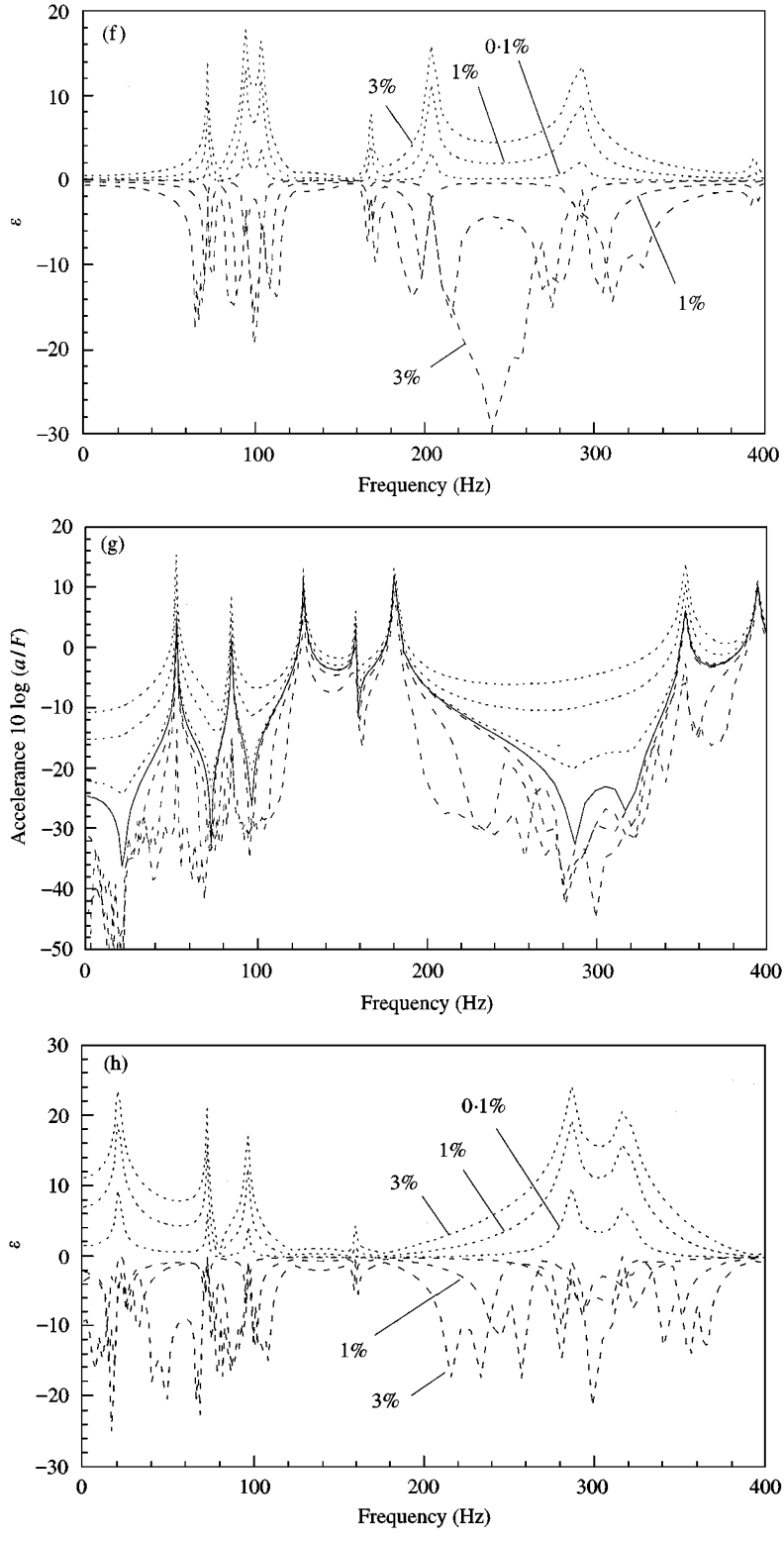

Figure 7. Continued

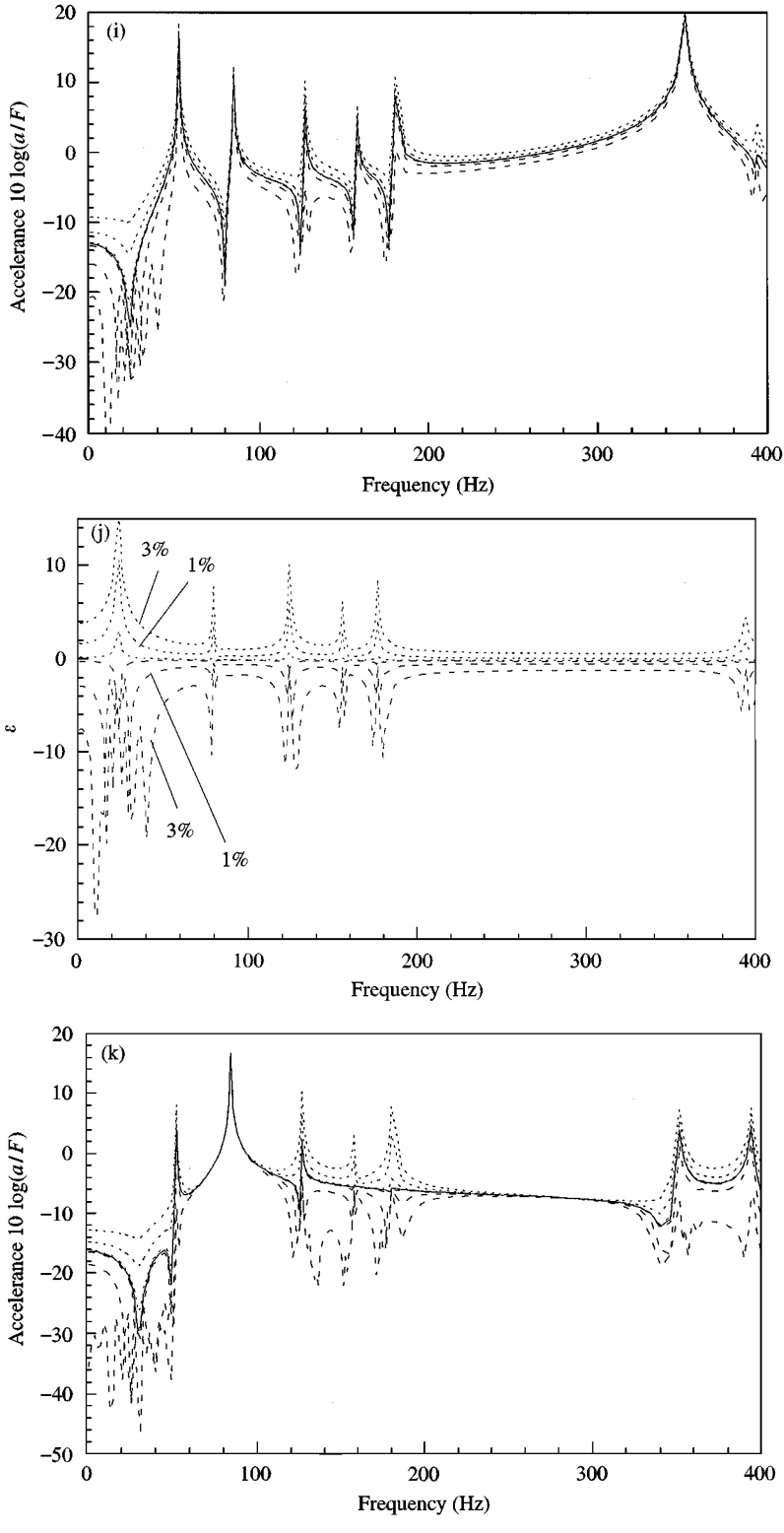

Figure 7. Continued

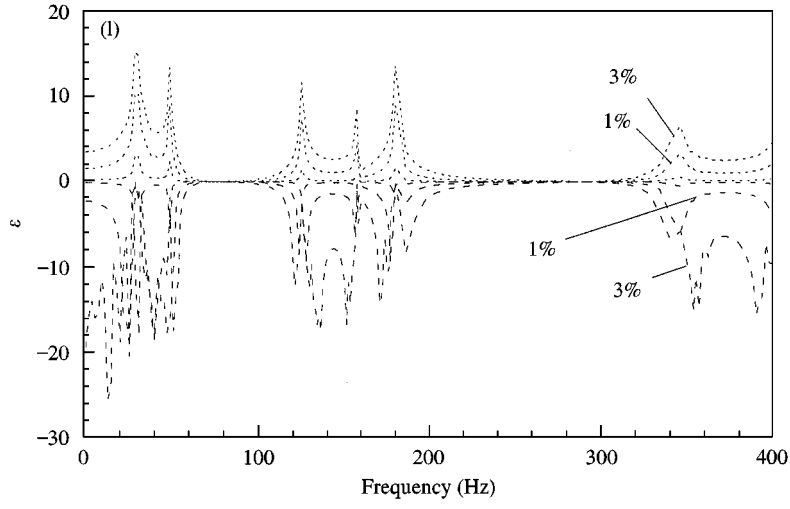

Figure 7. Continued

is low in comparison to the acceleration in the other directions. This problem usually occurs when there is an antiresonance in this direction or a resonance peak in one of the other directions. Consequently, those errors can be quite substantial as seen in Figures 7(e) to 7(h) or very small as seen in Figures 7(a), 7(b), 7(i) and 7(j). It is important to note that the angular and translational levels in Figure 7 are the results of combinations where the maximum sensitivity direction differs the most from the normal direction to the mounting surface at each frequency. This gives an estimation of the maximum error due to transverse sensitivities that can be expected in real measurements of this structure in this situation. It is also important to point out that these transverse sensitivity problems appear not only for the rotational d.o.f.s, but also for the translational d.o.f.s.

6. COMPARING CALCULATIONS WITH MEASUREMENTS ON THE TEST STRUCTURE

To check the performance of the actual prototype, the 6-d.o.f. transducer was mounted on the test structure, which was also calculated in FE. The measured accelerances can now be compared to the estimated (i.e., calculated) accelerances with different magnitudes of transverse sensitivities. In Figure 8, the measured accelerances are plotted with the estimated accelerances having 0% transverse sensitivity. Additional accelerances are shown where the transverse sensitivity magnitude is set to different values to give a similar fit to the measurement results.

By comparing the calculated and measured accelerances shown in Figure 8, it is possible to see the effects of the transverse sensitivity in many of the measured accelerances. For instance, the measured accelerance in Figure 8(d) has an increased magnitude in the range of 200–350 Hz, which corresponds well to an

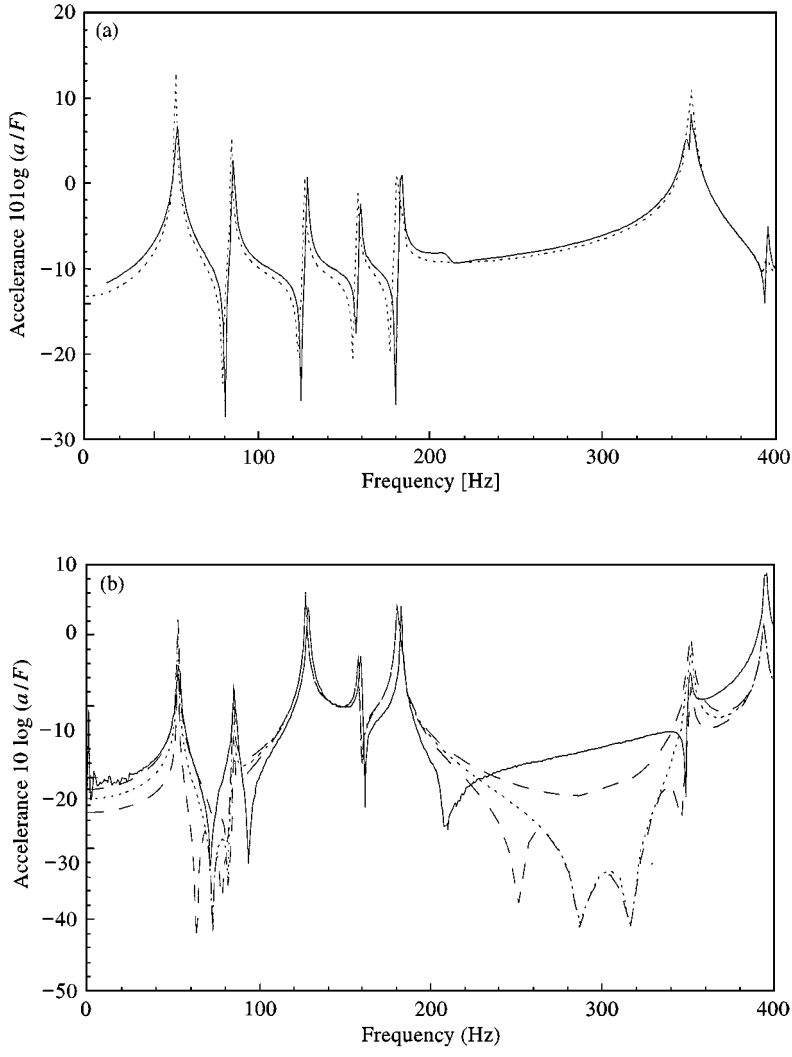

Figure 8. Measured (—) and theoretical accelerances using different sensitivities: (- - -) 0%. (a) x direction; (b) y direction (– – –) 3%; (c) z direction (– – –) 1%; (d) $\dot{\omega}_x$ direction (– – –) 1%; (e) $\dot{\omega}_y$ direction (– – –) 1%; and (f) $\dot{\omega}_z$ direction (– – –) 1%. Both positive and negative errors are indicated for most sensitivities.

estimated transverse sensitivity magnitude of 1%. In Figure 8(f), the extra peaks in the frequency range of 120–200 Hz can be seen to be caused by the transverse sensitivities of the accelerometers as well. It is also possible to see that there are some differences in the FE-model compared to the measured responses. For instance, the measured level in Figure 8(f), which is somewhat higher compared to the FE-model in the frequency range of 200–400 Hz, is probably due to the antiresonance frequency occurring on the other side of the resonance frequency of 340 Hz. This model problem might be due to the fact that the corner is welded, and the irregularities from the welding are not present in the FE-model.

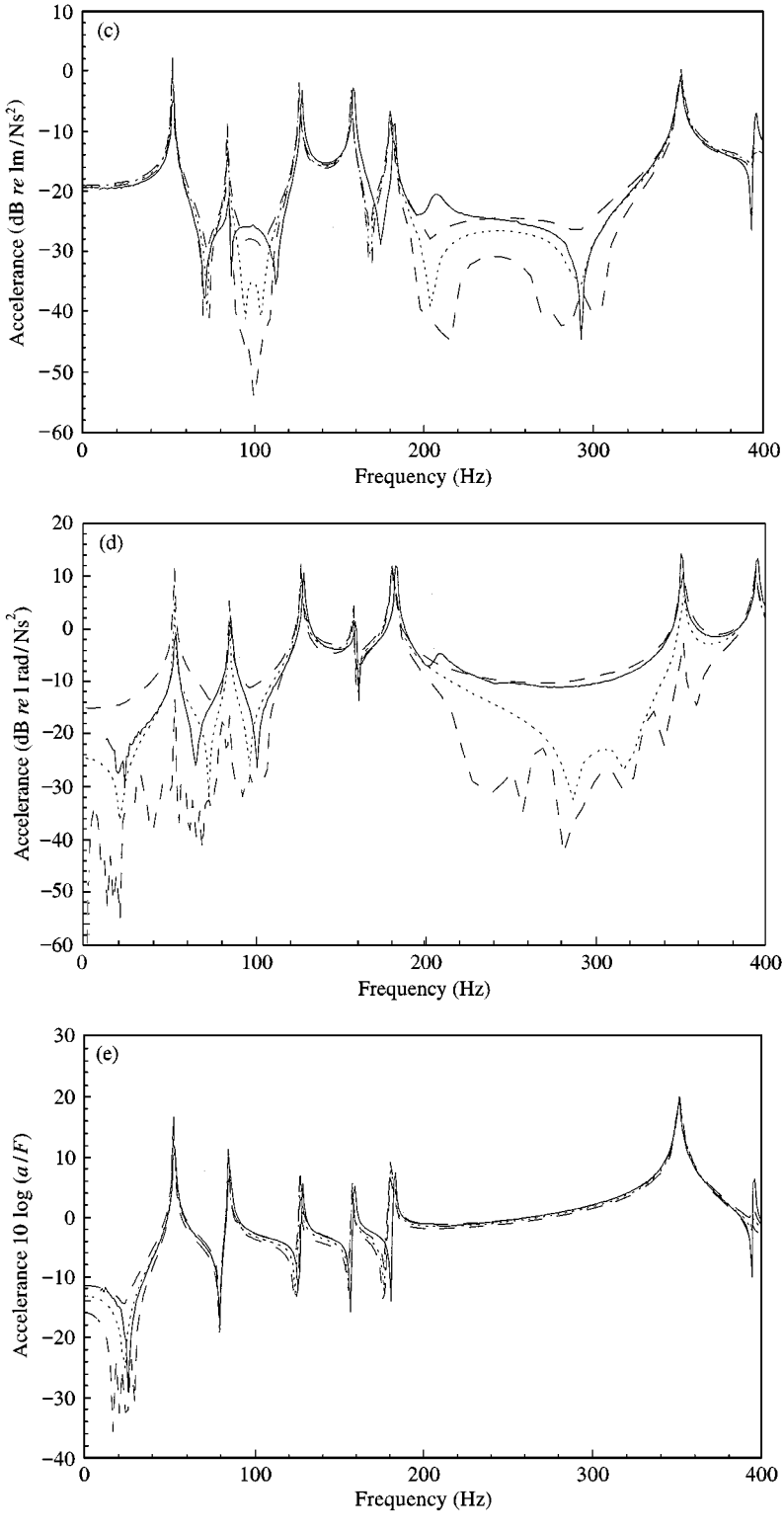

Figure 8. Continued

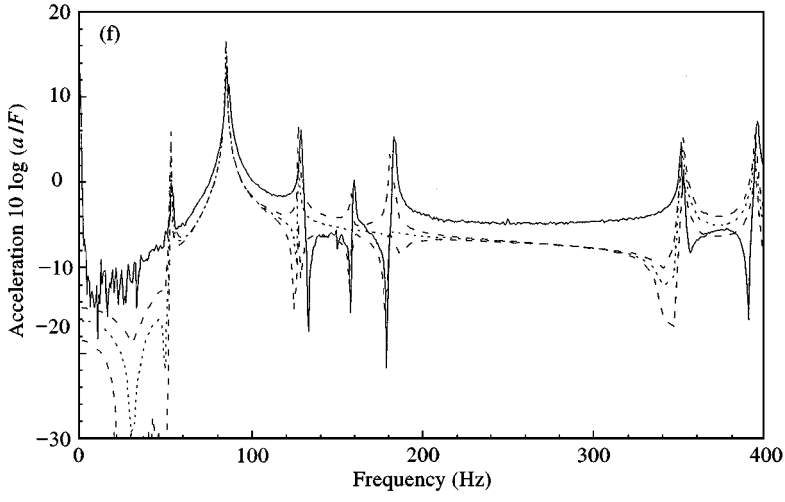

Figure 8. Continued

7. DISCUSSION OF THE THREE PARTS OF EXPRESSIONS (4)–(9)

The theoretical model of the structure allows the study of the different parts of expressions (4)–(9).

In order to understand the relative significance of these three parts, their contributions can be compared with each other. In Figure 9 the magnitudes of the three parts are plotted. The third part appears in the case considered here to be less important than the other two parts.

Removing part 3, giving simplified versions, can therefore reduce expressions (4)–(9). Using the measured accelerations, the influence of transverse sensitivity (part 2) can be determined. This is shown in Figure 10 where only measured data is used and a transverse sensitivity of 1% is assumed.

As seen in Figure 10(a), the transverse sensitivity components play a small role compared to the total measured accelerance. In another case, for example, as seen in Figure 10(d), the transverse components can dominate the measured accelerance at some frequencies.

8. LOW- AND HIGH-FREQUENCY LIMITS

When using two accelerometers to measure the rotation according to Figure 1 a finite difference approximation is carried out. This implies that $\alpha_o = \Delta y/\Delta x$ for small Δx. Δx is the spatial distance between the accelerometers and Δy the difference in acceleration between the two accelerometers.

To study the error due to this approximation, a test function $y(x) = \sin(k_x x)$ with $k_x = 2\pi/\lambda_s$ is used. The angle at $x = 0$ is calculated exactly and by a finite difference approximation with symmetrically spaced calculation points around zero for positive and negative values of x. The error is calculated as $10 \log 1 + \varepsilon(\alpha)$ where $\varepsilon(\alpha) = (|\alpha_{\text{finite difference}}| - |\alpha_{\text{correct}}|)/|\alpha_{\text{correct}}|$. The result from this calculation is shown in Figure 11, as the curve with zero-phase error.

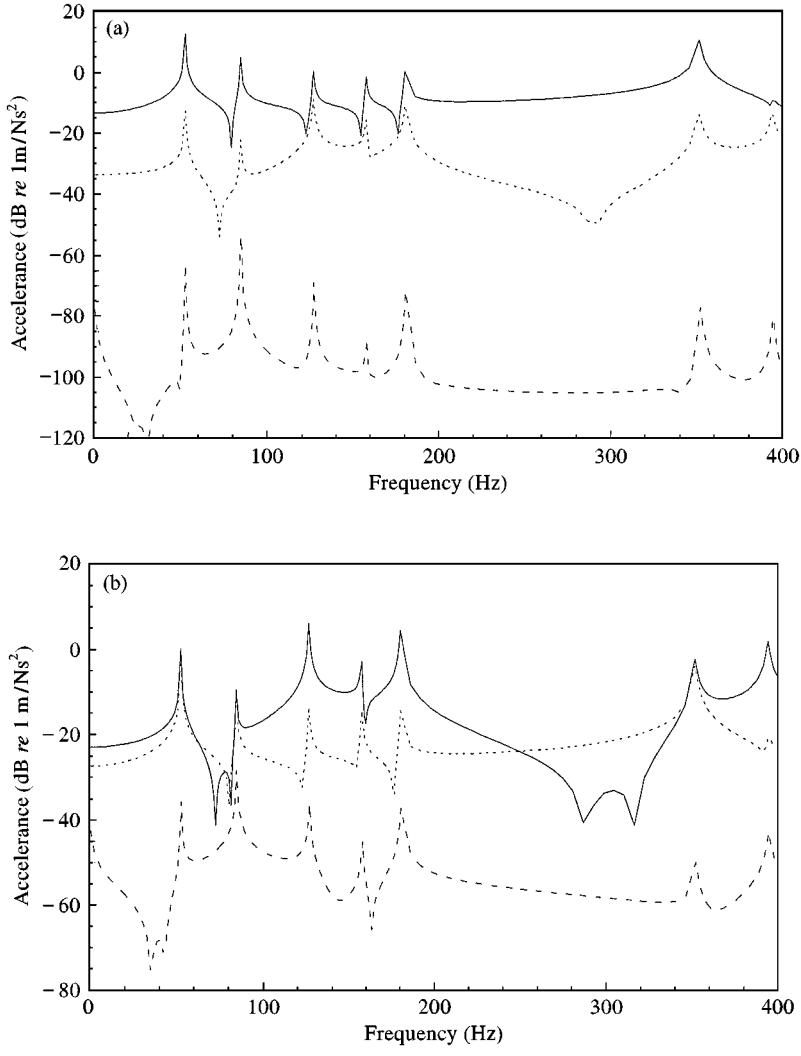

Figure 9. The three parts of expressions (4)–(9): (—) part 1, (- - -) part 2 and (– – –) part 3. (a) x direction; (b) y direction; (c) z direction; (d) $\dot{\omega}_x$ direction; (e) $\dot{\omega}_y$ direction; (f) $\dot{\omega}_z$ direction.

Many accelerometers have a specified low-frequency limit depending on the low-frequency sensitivity. For those accelerometers used in this work, limits are specified down to 20 Hz. The phase error for the accelerometers and the analyzer is of the order of 0·5° or smaller in the low-frequency range depending on the equipment used. Besides this, there is an additional factor influencing the low-frequency limit of the 6-d.o.f. transducer itself. When measuring rotations, by taking differences of acceleration signals, the sensitivity for phase errors arises when the phase difference between the accelerations becomes of the same order as the phase error in the complete measurement chain. This is a problem in the low-frequency region when the wavelength is much longer than the distance between the accelerometers.

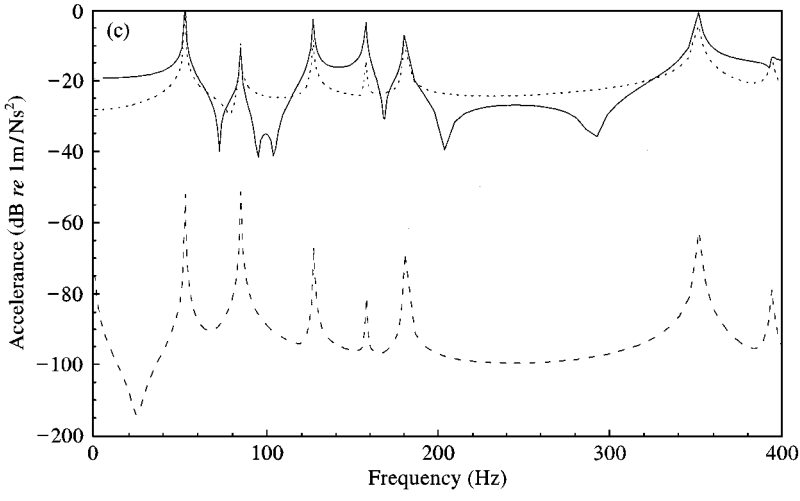

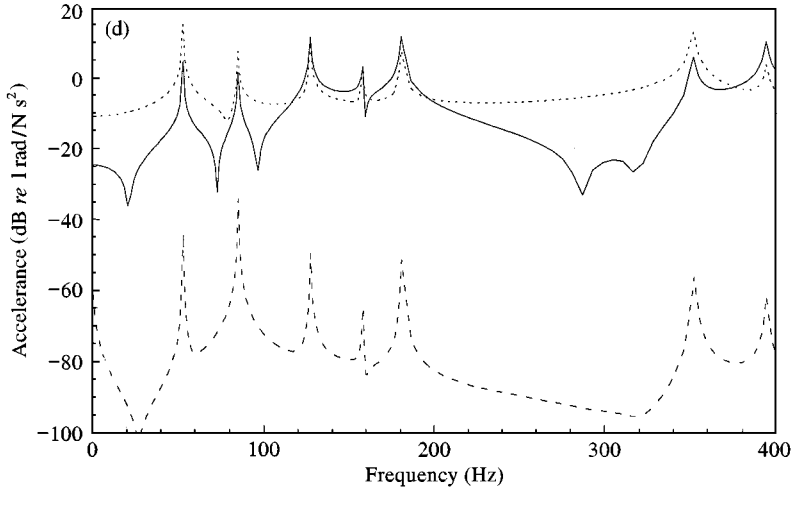

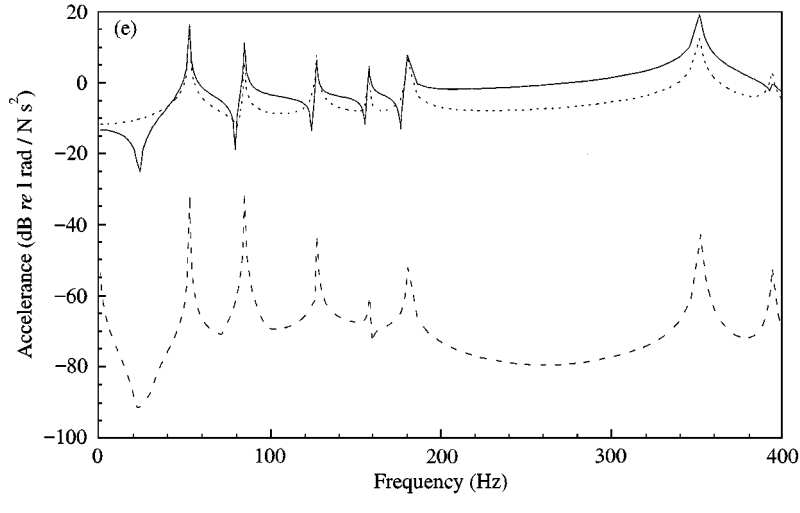

Figure 9. Continued

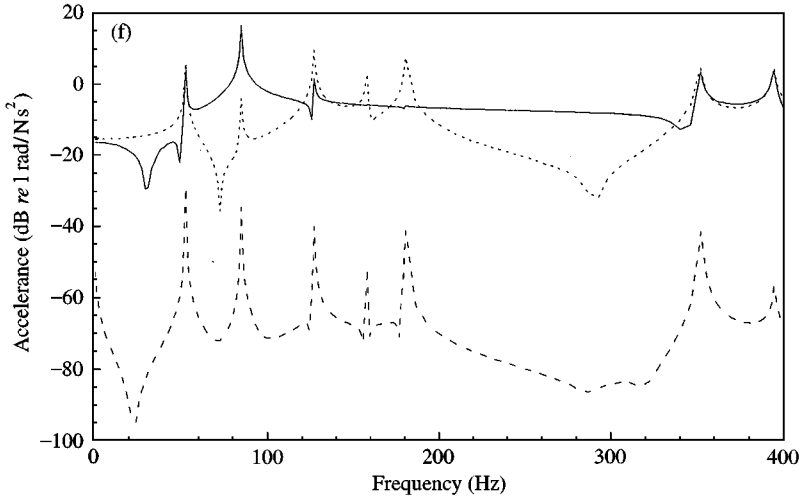

Figure 9. Continued

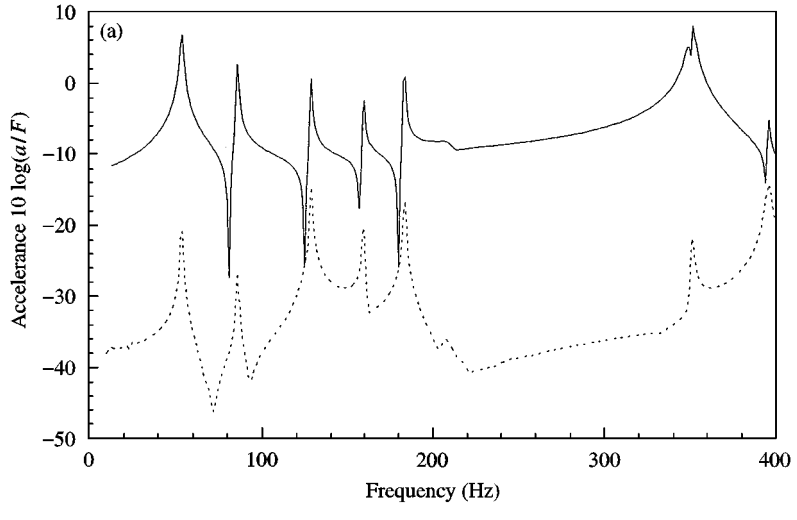

Figure 10. Part 2 (- - -) of expressions (4)–(9) compared with the total (—) accelerance using measured data. (a) x direction; (b) y direction; (c) z direction; (d) $\dot{\omega}_x$ direction; (e) $\dot{\omega}_y$ direction; (f) $\dot{\omega}_z$ direction.

The effect of phase error is studied with the same test function as the before. $z(x) = \sin(k_x x)$ with $k_x = 2\pi/\lambda_x$ being the wave number in the x direction. A phase error is easily added to the finite difference calculation function.

The errors of the rotational magnitude, α, due to a phase error of 1, 0·5, 0·1 and 0° are plotted in Figure 11.

If a rotational magnitude error of 1 dB is acceptable for a rotational d.o.f. measurement, then the quotient of the distance between the accelerometers and the wavelength, $2L/\lambda$, must be in the range $0{\cdot}006 < 2L/\lambda < 0{\cdot}41$ in order that the phase

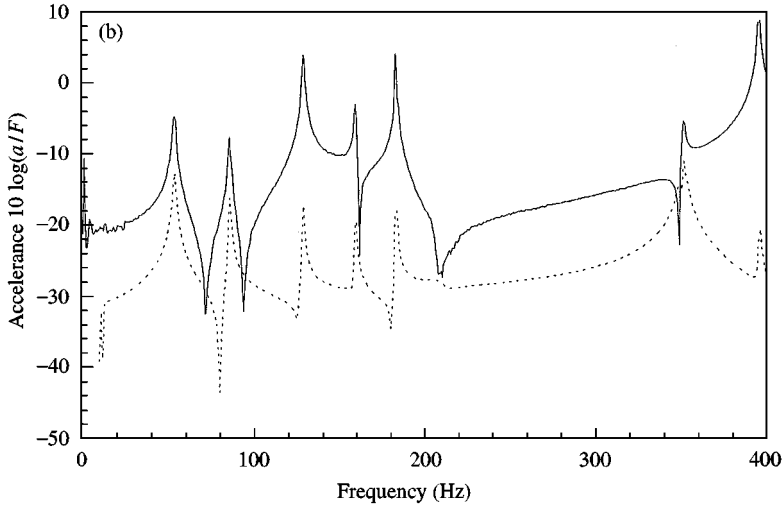

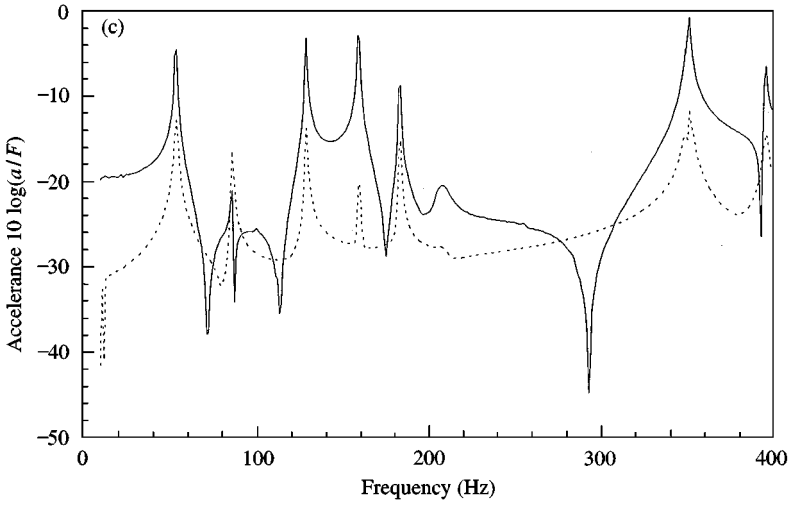

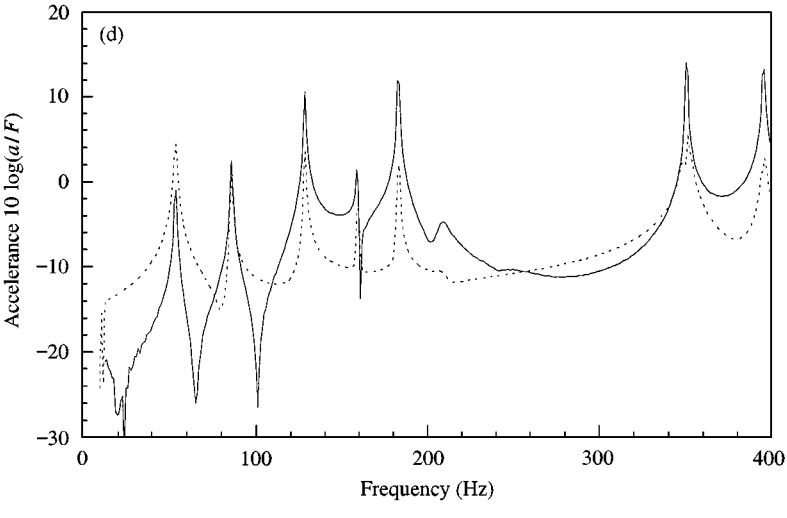

Figure 10. Continued

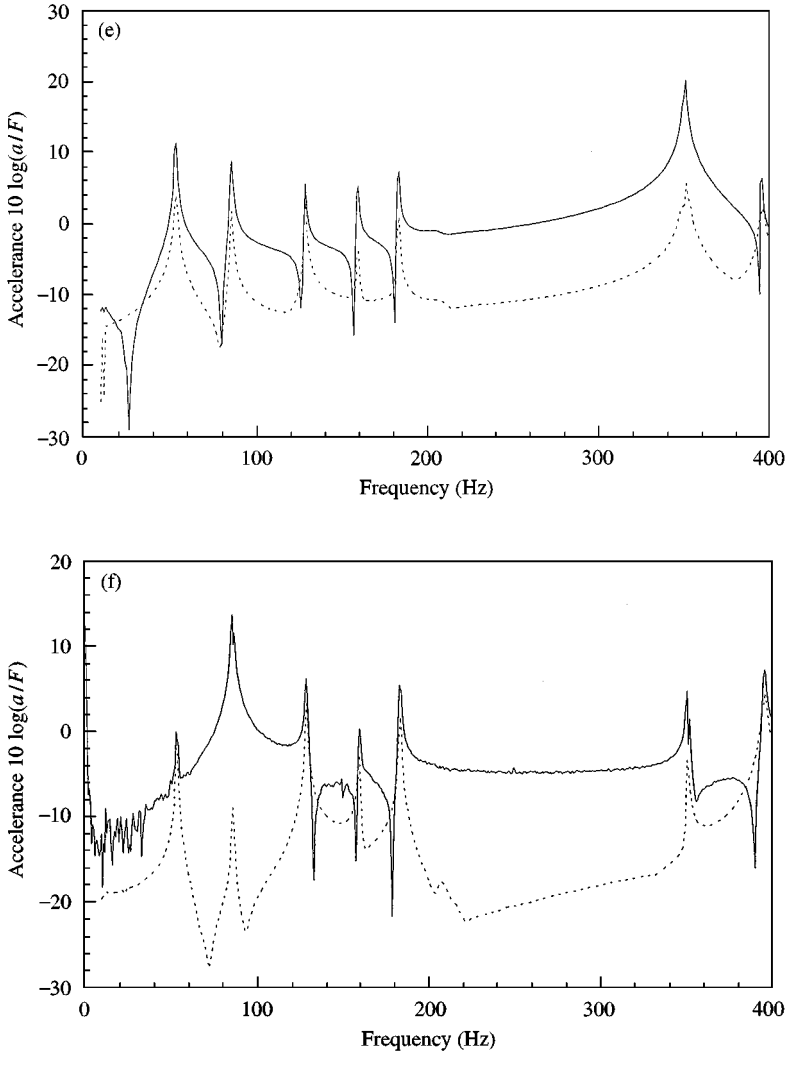

Figure 10. Continued

error is smaller than 0·5° in the complete measurement chain. The transducer tested here has $2L = 0{\cdot}02$ m which gives measurable wavelengths between 3·3 m and 49 mm with an error less than 1 dB if a phase error smaller than 0·5° can be assumed.

The high-frequency limits of the transducer are mainly determined by three factors. Firstly, there is the finite difference approximation as previously discussed, secondly, there is an upper limit defined by the mounting resonance frequency of the accelerometer itself, in this case about 17 kHz and thirdly there is the first fundamental resonance of the transducer depending on its weight and stiffness. For the design used in this paper, the first eigenfrequency of the fixture is about 6 kHz; see Figure 12. This resonance seems to limit in our case the applicability of the transducer. In Figure 13, measurements on a simple beam are compared with

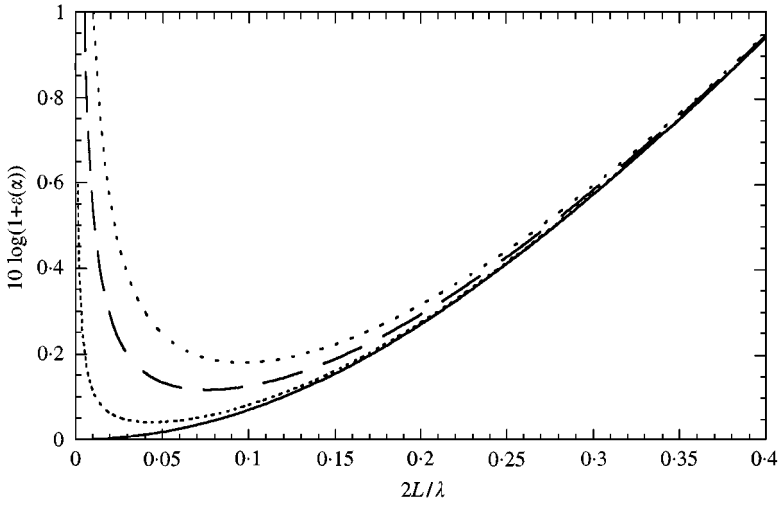

Figure 11. The bias error of the rotational magnitude as a function of $2L/\lambda$ (distance between accelerometers divided by wavelength), due to finite difference approximation and phase errors of (—) 0°, (· · ·) 0·1°, (– – –) 0·5° and (- - -) 1°.

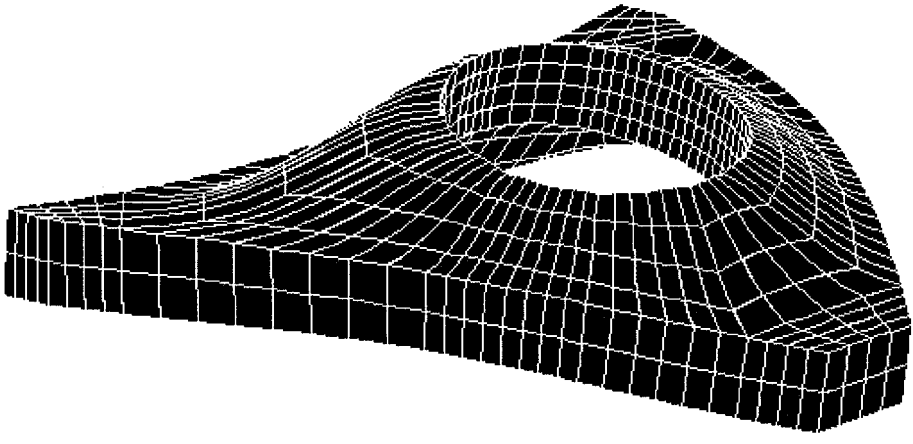

Figure 12. First eigenmode of the 6-d.o.f. transducer at 6·071 kHz.

analytical calculations. The magnitude error starts to grow at one-third of the fundamental resonance frequency (about 2 kHz). The phase error is already visible at 1/10 of the resonance frequency (about 600 Hz). However, FE-studies have shown that it is possible to increase the transducer's first eigenfrequency up to at least 10 kHz by reinforcements.

9. SENSITIVITY

When performing a six-d.o.f.s measurement, it is important to have transducers that are sufficiently sensitive regarding the vibration amplitudes of the measurement object. Usually, the sensitivity of a piezo-crystal accelerometer

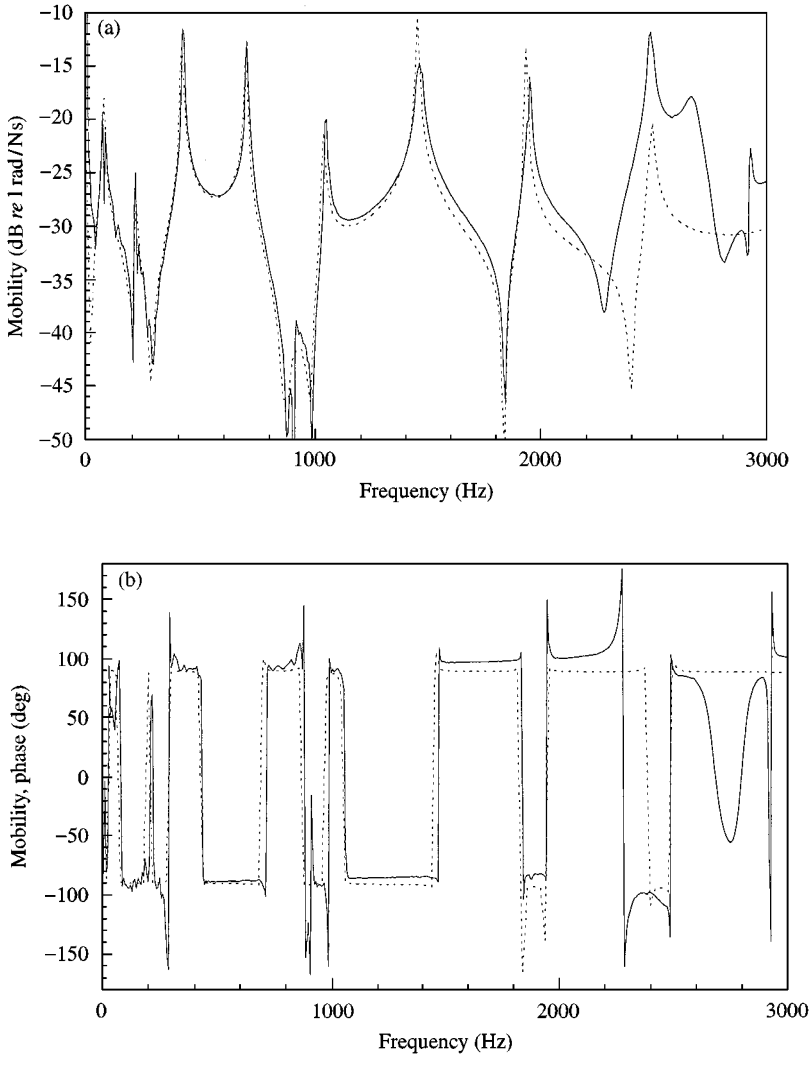

Figure 13. Mobility magnitude and phase of a free–free beam: (—) measured and (- - -) calculated.

increases with increasing seismic mass. However, this increases the total mass and decreases the high-frequency limit of the transducer. It is important to have a low transducer mass to avoid mass loading. The accelerometers used for this 6-d.o.f. transducer are of ICP-type, i.e., they have a built-in amplifier and impedance converter. The sensitivity for a 0·2 g accelerometer of the ICP-type is typically 5 mV/g. This value can be compared with a 2·3 g shear type accelerometer which has a sensitivity of 3 mV/g. The angular sensitivity can be calculated from the sensitivities of each accelerometer and by the distance between them. For the 6-d.o.f. transducer this gives the value of about 0·01 mV s^2/rad. There are mainly two ways of increasing the sensitivity of the transducer, by using accelerometers with high sensitivity or enlarging the distance between the accelerometers. The first

way requires normally an increase of the seismic mass leading to a heavier transducer with a lower mounting resonance frequency and a higher mass loading. The second way of increasing the transducer sensitivity is by enlarging the distance between the accelerometers, which also leads to a higher transducer mass and will decrease the high-frequency limits.

10. DISCUSSION

The equations of motion were established including transverse sensitivity. Comparisons between calculations and measurements show the importance of transverse sensitivity terms. The influence of transverse sensitivity is large at antiresonances or when there exists high-vibration amplitudes in other directions.

Measurements can be used to study the influence of the transverse sensitivity.

For high-precision measurements there is a need to know the transverse sensitivity in magnitude and phase for all accelerometers used in the estimation. If this is known one can compensate measurements, but then all 6-d.o.f.s have to be measured.

The transducer design has to be optimized with regard to weight/stiffness ratio such that its first structural resonance determines the upper frequency of applicability. The version used here has a fundamental resonance of 6 kHz, which gives a phase error of about 2° at 600 Hz. The low-frequency limit is around 4·2 m in wavelength or at 20 Hz, if the signal-to-noise ratio is sufficiently large.

The transducer has a low mass, which is important when measuring on lightweighting structures. The transducer is flat which makes it possible to measure responses close to a surface and to have the possibility to place it between a structure and isolator in some cases. The transducer has a hole in the center to give the possibility of measuring *true* point mobilities by applying a force or moment there. *True* in this case means that the force or moment excitation is positioned at the same point as the response and not some small distance apart, which is very common, unless an impedance head is used.

ACKNOWLEDGMENTS

This work has been financially supported by the Swedish Research Council for Engineering Sciences (TFR) through contract 95-160 and the Swedish Council for Building Research (BFR) through contract 950192-8.

REFERENCES

1. D. H. Soyster and M. W. Trethewey 1996 *Journal of Analytical and Experimental Modal Analysis* **11**, 76–82. Use of rotational elements in structural dynamic modification.
2. D. J. Ewins and M. G. Sainsbury 1972 *The Shock and Vibration Bulletin* **42**, 105–122. Mobility measurements for the vibration analysis of connected structures.
3. M. A. Sanderson 1996 *Journal of Sound and Vibration* **198**, 171–191. Vibration isolation: moments and rotations included.

4. Y. K. KOH and R. G. WHITE 1996 *Journal of Sound and Vibration* **196**, 509–522. Analysis and control of vibrational power transmission to machinery supporting structures subjected to a multi-excitation system, Part 3: vibrational power cancellation and control experiments.
5. B. A. T. PETERSSON 1996 *Journal of Sound and Vibration* **196**, 295–321. Concentrated excitation of structures.
6. J. LEE and P. W. WHALEY 1976 *Journal of Sound and Vibration* **49**, 541–549. Prediction of the angular vibration of aircraft structures.
7. D. J. EWINS 1984 *Modal Testing: Theory and Practice*. Taunton, Somerset, England: Research Studies Press, reprint 1995.
8. T. R. LICHT 1985 *Proceedings of the 3rd IMAC, Orlando*, 503–506. Angular vibration measurements. Transducers and their configuration.
9. R. A. L. RORRER, A. L. WICKS and J. WILLIAMS 1989 *Proceedings of the 7th IMAC, Las Vegas*, 1300–1304. Angular acceleration measurements of a free–free beam.
10. M. W. TRETHEWEY, H. J. SOMMER and J. A. CAFEO 1993 *Journal of Sound and Vibration* **164**, 67–84. A dual beam laser vibrometer for measurement of dynamic structural rotations and displacements.
11. C. HO 1991 *Dissertation. Rensselaer Polytechnic Institute, Troy*, New York: Experimental and theoretical investigation of a six-degree-of-freedom translational-rotational accelerometer sensor.
12. J. L. MERIAM 1980 *Engineering Mechanics Statics and Dynamics*. New York: John Wiley & Sons. ISBN 0-471-06156-5.
13. M. SERRIDGE and T. R. LICHT 1986 *Brüel & Kjaer*. Glostrup: K. Larsen & Søn A/S-DK-2600. Piezoelectric accelerometers and vibration preamplifiers, theory and application handbook.

APPENDIX A

Some measurements have been performed at Bosch, for the European Brite Euram project "QUATTRO" BE 97-4184, using their laser doppler vibrometer (LDV). These measurements were made to see if it is possible to use a laser to determine the transverse sensitivities of transducers using a common shaker. Two

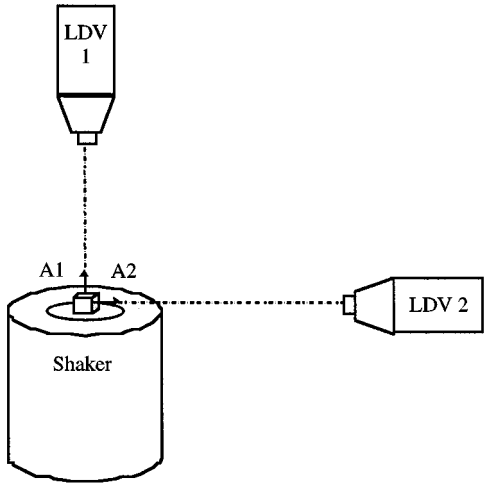

Figure A1. Test set-up used for measuring the transverse sensitivity.

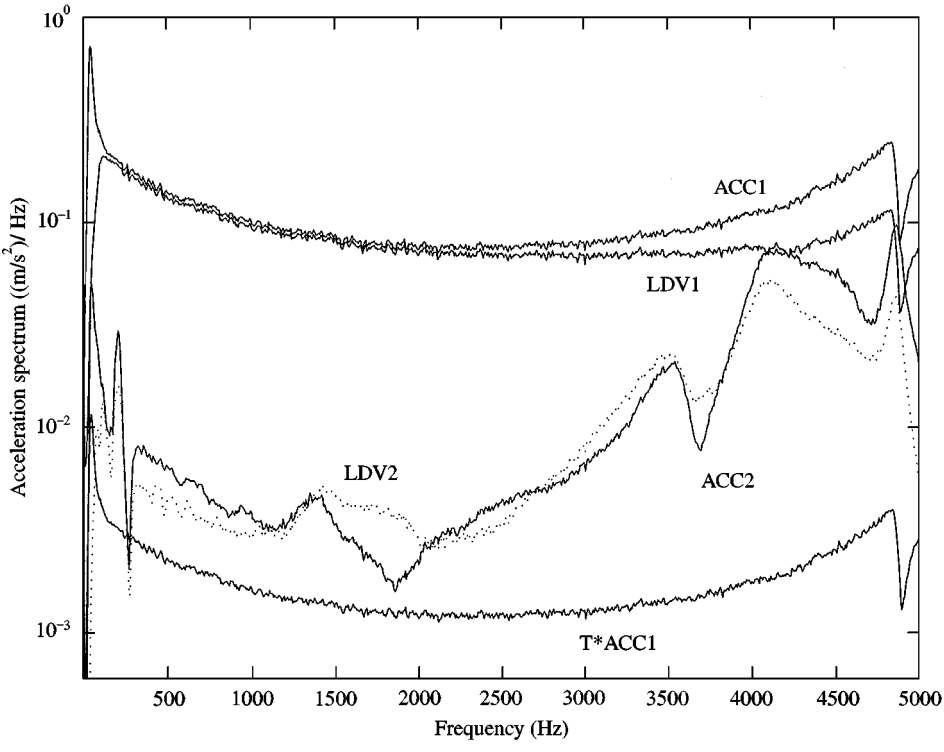

Figure A2. The different acceleration spectra measured on the top of the shaker with both laser and traditional accelerometers in the main direction and in the transverse direction. The frequency resolution was 6·25 Hz.

small (0·2 g) accelerometers, ACC1 and AAC2, were mounted on a specially made cube which was mounted on top of a shaker according to Figure A1.

The two accelerometers had the specified transverse sensitivities of 1·6% (respectively 1·8%) according to the manufacturer. The acceleration in direction A1 was measured with LDV1 and with accelerometer ACC1. The acceleration perpendicular to direction A1, namely A2, was measured with LDV2 and accelerometer ACC2. The shaker was driven with a white noise spectrum up to 5 kHz. The results from the measurements are seen in Figure A2.

Also shown in Figure A2 is a curve marked T*ACC1 which is the transverse sensitivity of the accelerometer (given by the manufacturer) multiplied by the acceleration in the A1 direction. As seen, the LDV and the accelerometers give almost the same results, the difference is probably not due to the transverse sensitivity.

As long as the two curves marked LDV2 and ACC2 have a greater magnitude than the curve marked T*ACC1, then the set-up is not good enough to use in order to determine the frequency-dependent transverse sensitivity of these accelerometers.

In other words, the shaker is not moving unidirectionally and the motions in other directions, other than the main direction, are greater than 1·8% of the main direction at all frequencies.

Therefore, this measurement set-up cannot be used to determine the transverse sensitivities of accelerometers.